Stabilizing Control of a Urine Nitrification Process in the Presence of Sensor Drift

Christian M. Thürlimann[a,b], Kai M. Udert[a,b], Eberhard Morgenroth[a,b], Kris Villez[a,b,*]

[a]Eawag, Überlandstrasse 133, CH-8600 Dübendorf, Switzerland
[b]ETH Zürich, Institute of Environmental Engineering, 8093 Zürich, Switzerland

Abstract

Sensor drift is commonly observed across engineering disciplines, particularly in harsh media such as wastewater. In this study, a novel stabilizing controller for nitrification of high strength ammonia solutions is designed based on online signal derivatives. The controller uses the derivative of a drifting nitrite signal to determine if nitrite-oxidizing bacteria (NOB) are substrate limited or substrate inhibited. To ensure a meaningful interpretation of the derivative signal, the process is excited in a cyclic manner by repeatedly exposing the NOB to substrate-limited and substrate-inhibited conditions. The resulting control system successfully prevented nitrite accumulations for a period of 72 days in a laboratory-scale reactor. Slow disturbances in the form of feed composition changes and temperature changes were successfully handled by the controller while short-term temperature disturbances are shown to pose a challenge to the current version of this controller. Most importantly, we demonstrate that drift-tolerant control for the purpose of process stabilization can be achieved without sensor redundancy by combin-

*Corresponding author. Email kris.villez@eawag.ch

ing deliberate input excitation, qualitative trend analysis, and coarse process knowledge.

Keywords: nitrite control, inflection point, shape constrained splines, relative measurement, online experiment, nitrification

1. Introduction

Control loops relying on absolute sensor values often suffer from sensor faults. This study presents a novel control concept to stabilise a reactor for nitrification of high strength ammonia solutions in the presence of sensor drift. To this end, the controller is designed to exploit information from the signal derivatives in a deliberately excited process. In wastewater, biological, chemical, and physical factors lead to particularly intense wear and tear of sensors. Hence, even mature sensor hardware such as pH sensors still exhibit drift when exposed to this harsh medium. This drift occurs at time scales that are much longer than typical process dynamics, challenging a comparison with the sensor data history (temporal redundancy) (Ohmura et al., Submitted). Furthermore, drift tends to occur in all sensors exposed to the same medium challenging its detection based on redundant placement of sensors (spatial redundancy). Lack of spatial and temporal redundancy impedes the application of tools such as active fault tolerant control that correct drift automatically based on redundant information (Blanke et al., 2016).

The root causes of sensor drift are generally assumed to be known well

- e.g., biofilm formation, salt deposition, electrode oxidation etc. - but are typically hard to quantify. There are a few attempts to investigate drift of sensors quantitatively by controlled offline experiments (Ohmura et al., Submitted) or by online experiments (Samuelsson et al., 2018). However, drift is typically identified by means of on-site manual reference measurements in practice. This makes drift expensive to detect and correct, particularly when remote or decentralised systems are considered.

The limited capacity to quantify sensor drift in wastewater processes on the one hand and the need to control these processes on the other hand, led to the development of methods that disregard absolute sensor values and extract information that is represented in the derivatives of the sensor signal. The most discussed (soft-)sensor signals that reveal relevant information without relying on a classical notions of accuracy are pH, oxidation-reduction potential (ORP) (Al-Ghusain et al., 1995), and oxygen uptake rate (Baeza et al., 2002). Al-Ghusain et al. (1995) used the derivatives of pH and ORP to operate an aerobic/anoxic sludge digestion reactor. In these cases, the sequenced operation creates the dynamics in the recorded sensor signals that enable information extraction. In continuously operated processes, trend-based monitoring and control is possible thanks to naturally occurring periodicity of the (unmeasured) process input disturbances (e.g. hydraulic load, nitrogen load, Thürlimann et al., 2018).

The application of trend-based control concepts is expected to be more challenging in systems without naturally occurring disturbances. The source-separated collection and nitrification of anthropogenic urine for the purpose of fertilizer recovery is an example of such a system. Separated collection of undiluted urine at the building or household level enables to smoothen the hydraulic load with a small buffer tank. Our experience (not shown) suggests that short-term storage of anthropogenic urine does not affect the total nitrogen concentration, meaning that the naturally occurring variations in the nitrogen load to a nitrifying reactor are expected to be small. Despite the apparent lack of input disturbances, the process is sensitive to inadvertent nitrite accumulation events, which cause a complete failure of the process in absence of corrective actions (Fumasoli et al., 2016; Sun et al., 2012).

An economically viable method to measure nitrite online is UV-Vis absorbance spectrophotometry. However, this measurement principle lacks specificity and therefore needs a model to extract the nitrite concentrations from the absorbance measurement. Despite the availability of robust hardware, extrapolation of such models makes drift of the nitrite signal a very likely phenomenon (Gruber et al., 2006; Brito et al., 2014; Etheridge et al., 2014), as is also demonstrated below.

The lack of natural or operational dynamics, the presence of signal drift, and the open-loop unstable process of urine nitrification motivates the development of a specialized control concept. This control concept, as explained in detail below, extracts the essential information needed to prevent dangerous nitrite accumulation events by means of *(i)* deliberate induction of process dynamics (excitation) and *(ii)* trend analysis of a drifting sensor signal. In turn, this information extraction process enables the construction of single-in-single-out (SISO) controller for stabilization of the urine nitrification process.

2. Material and methods

2.1. Conceptual model of the control problem

In this paragraph, a conceptual model of the urine nitrification process is presented. The concept illustrates the different process states (Gujer, 2008), growth rate of the ammonia oxidizing bacteria (μAOB) and growth rate of the nitrite oxidizing bacteria (μNOB) and connections indicating the causal relationships between these variables and the sign of the magnitude of each influence (positive/negative influence). In the control literature, these signs are known as the signs of gains (Åström and Murray, 2008). It is important to note that this conceptual model only includes the effects considered relevant to tackle the identified process stabilization challenge. Only dynamic effects with a lower time constant than the controller are considered (e.g., biomass concentration stays approximately constant within this time scale). In addition, direct inhibition of the AOB and NOB activity by ammonia is considered marginal in the studied operational region (pH 5.9 to 7.0). The indicated signs of gains are only valid if all other states and rates remain constant and under constraints given in Fig. 1.

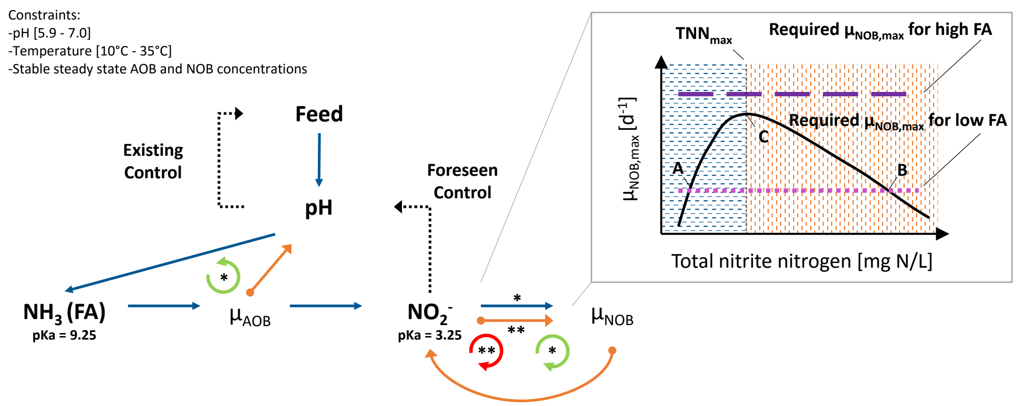

Figure 1: Conceptual model of urine nitrification. Left panel: Process states, growth rates, and gains. Blue arrows: positive gains; orange arrows with dot: negative gains; Green arrows: negative feedback loop; Red arrows: positive feedback loop. Right panel: Nitrite oxidizing bacteria growth rate (μNOB) as a schematic function of total nitrite nitrogen concentration. Low nitrite concentration (blue dashes): NOB substrate limited; High nitrite concentration (orange dashes): NOB substrate inhibited. The top (bottom) horizontal line indicates the required μNOB to oxidise all the nitrite produced by the AOB given a high (low) free ammonia concentration.

The blue arrows indicate a positive gain, the orange dot-arrows indicate a negative gain of the connected elements. For example, an increasing loading rate leads to an increased pH (i.e., positive gain) and an increasing AOB rate (μAOB) leads to a decreased pH (i.e., negative gain). The gains can create loops. Such loops are open loop stable if the product of the gains is negative (e.g., pH - NH_3 - μAOB) (green/* circle arrows). This means these loops are self-stabilizing. For example, an incrase of the pH due to a process disturbance (e.g. higher hydraulic load, higher pH of influent) will increase the free ammonia (NH_3 or FA) concentration in the bulk, which in turn raises the μAOB. In turn, this decreases the pH, therefore stabilising this part of the process. A loop with a positive product of its gains is a positive feedback loop and can lead, when not controlled properly, to a complete disappearance of elements in the loop (i.e., open loop unstable).

In the present case, nitrite has a negative gain to μNOB when the nitrite concentrations are high (i.e., orange arrow). A high nitrite concentration reduces the nitrite oxidation rate. This increases the net nitrite production rate in turn inducing to an even stronger inhibition of the NOB. Eventually, this leads to NOB wash-out and process failure. This part of the process is open loop stable if the nitrite concentration remains low (i.e. blue arrow). Under such circumstances, marginal increases of the nitrite concentration increase the NOB activity, which decreases the net nitrite production rate. Practically, the process can only be stabilised by reducing the AOB activity whenever the nitrite concentration reaches NOB-inhibiting levels. This is possible by making the reactor anoxic, in which case nitrite is reduced by denitrification. This may induce growth of denitrifiers however, in turn leading to a loss of nitrogen to the environment. For the purpose of fertilizer production, a better approach consists of reducing the nitrite production rate by decreasing the pH setpoint. Low pH values induce lower FA concentrations, so that eventually the nitrite oxidation rate is higher than the nitrite production rate (Fig. 1 right).

More details concerning the influence of the ${NO_2}^-$ concentration on the

NOB activity (μNOB) are shown in the top right box of Fig. 1. It shows μNOB as a function of the total nitrite concentration (TNN) (full line). The growth rate is composed of both the substrate limiting effect and the inhibition effect nitrite has on the NOB. Most studies, but not all, list nitrite as the substrate and free nitrous acid (FNA) as the inhibiting substance for NOB (Park and Bae, 2009). This means that the growth rate is pH dependent. For simplicity, we neglect any effect of the pH and assume that TNN is both the substrate and the inhibitory substance. In practice the exact value of the TNN concentration where the effect of substrate inhibition overpowers the effect of substrate affinity is known only coarsely due to a variety of factors. These include process-related factors such as *(i)* the incompleteness of available knowledge describing the influences of biomass composition, urine composition, and temperature on the observed nitrite affinity and nitrite inhibition effects (van Hulle et al., 2007) and *(ii)* insufficient accuracy and precision of laboratory concentration measurements to determine the critical nitrite concentration precisely, even under otherwise stable conditions.

The black dashed arrows indicate the existing pH control loop as well as the newly proposed nitrite control loop for process stabilization. The pH control loop is described below and is designed to protect the AOB from washout (cf. 2.2.3). The second dashed arrow indicates the proposed master control of the pH control loop in the reactor based on the nitrite concentration, which is aimed at preventing washout of the NOB.

2.2. Basic reactor set-up and operation

The reactor used for this study is a cylindrical 12 L continuous flow stirred tank reactor (CSTR) nitrifying source-separated urine. The hydraulic retention time (HRT) of the reactor system varied between 7 and 13 days, as is discussed below. The reactor was operated without biomass retention so that the sludge retention time (SRT) equals the HRT. The reactor was in operation since 19 months prior to the start of this study. The reactor includes two recirculation loops. One brings the reactor medium to the UV-Vis spectrophotometer with a HRT of 10 s. The other brings medium to a pH sensor pack used in another study (HRT: 20 s, Ohmura et al., Submitted). The feed composition is described in 2.5.3. The available alkalinity limits the fraction of the total ammonium converted via nitrite to nitrate to roughly 50% (detailed results below).

2.2.1. Analytics

Samples are taken regularly from the reactor to evaluate if the proposed controller keeps the nitrite concentration low. To measure chemical species the following steps are executed. Per sample at least 2 ml of reactor media are filtered with 0.45 μm GF/PET filter (Art. Nr. 916 02, Macherey-Nagel, Oensingen, Switzerland) mounted on a sampling syringe. Ammonium, nitrite, and nitrate concentrations are measured in every sample. The influent ammonium and chemical oxygen demand (COD) concentrations are measured each time the influent tank was replaced. The exchange dates and concentrations are listed in the Electronic Supplementary Material (Table S1 and S2). Ammonium concentrations are determined either through a Metrohm 930 Compact IC Flex (Metrohm, Herisau, Switzerland, method: Metrohm Metrosep C6, 250/4.0), with flow injection analysis (FIA, Lachat QC8500, Hach Company, Loveland, USA) or with colorimetric test kits (LCK303, Hach-Lange, Berlin, as all LCK test kits). Nitrite reference concentrations are determined either colorimetrically with an LCK341 test kit or with strip tests (MQuant, Merck KGaA, Darmstadt, Germany) to confirm low nitrite concentrations. Due to dilution, the detection limit with the LCK341 kit is approximately 2 mg N/L. Nitrate is measured in the laboratory through a Metrohm 881 Compact IC Pro (Metrohm, Herisau, Switzerland, chemical suppression Metrosep A Supp 7, 250/4.0) or with an LCK340 kit. For the measurement of the COD, LCK314 kits are used. A standard deviation of the measurement including the dilution procedure is estimated with a single triplicate of measurements prior to this study: FIA ammonium: 0.60% at 2340 mg N/L, LCK 341 nitrite: 0.60% at 45.7 mg N/L, and IC nitrate: 0.55% at 2226 mg N/L.

2.2.2. Sensors

A 2 mm path length spectro::lyser V1 (s::can, Vienna, Austria) is used to measure the UV-Vis absorbance spectrum of the reactor content in-situ. The sensor measures the absorbance from 200 to 750 nm with a resolution of 2.5 nm. The *Ex-situ wBM* model from Thürlimann et al. (Submitted) is used to estimate the nitrite concentrations. Each minute a new absorbance measurement and in turn a new estimation of the nitrite concentration is obtained. Furthermore, two pH and two dissolved oxygen (DO) sensors are installed, one of each is used for control (DO: COS61D and pH: CPS11D, Endress&Hauser, Reinach, Switzerland)

2.2.3. Low-level control

The DO concentration is controlled between 5 and 6 mg O_2/L by on/off control of the airflow through a fine-bubble diffusor (6 L/min). The feed pump is pH controlled (cf. 2.3). The reactor is equipped with a water based heating/cooling system (FN-25, Julabo, Seelbach GmbH, Germany). The temperature of the reactor was controlled at 25°C with an accuracy of ±0.5°C due to diurnal variations unless stated otherwise.

2.3. Stabilizing Nitrite Control

The ultimate goal of our controller is to ensure that both AOB and NOB are retained and remain active in the studied reactor in the presence of typical disturbances. The envisioned control system has to ensure that the net nitrite production rate is zero, meaning that the ammonia oxidation is the rate-limiting step and that no ammonia is accumulating in the system. To this end, the master controller manages the nitrite oxidation (i.e., NOB) and the slave controller manages the ammonia oxidation (i.e., AOB). At the top of Fig. 2, the proposed cascaded control loops are illustrated. The slave control loop, using pH to control the inflow was described by Udert et al.

(2003). It controls the AOB by manipulating the inflow rate based on the pH setpoint given by the master control. The master control takes the nitrite concentration estimation as an indicator to decide if the ammonia oxidation rate is higher or lower than the theoretical maximum nitrite oxidation rate and sets the pH set point accordingly. The slave controller turns on the inflow pump when the pH drops below the pH setpoint. Instead of a higher second pH setpoint the pump is turned off again based on a timer (6 s). In each pump event 20 $\pm$ 5 mL of urine is fed to the reactor.

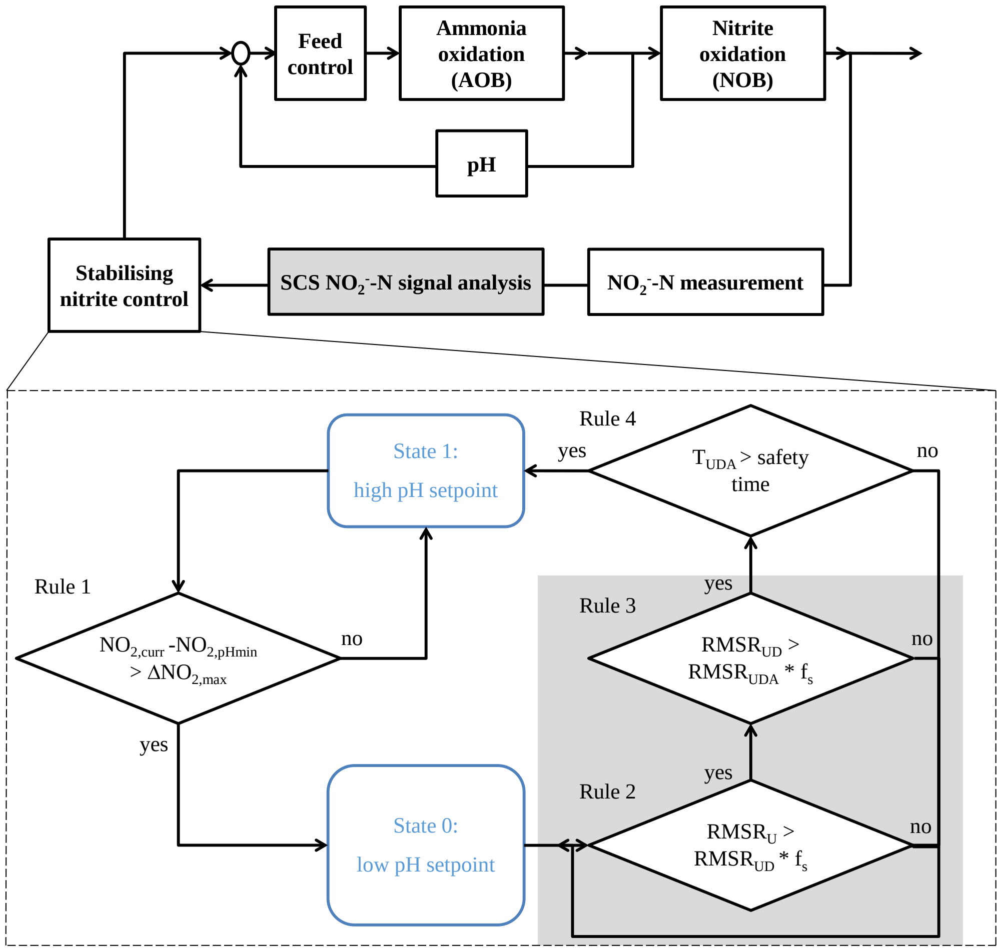

Figure 2: Control loops. Top: Cascade control of AOB and NOB. Bottom: rule based decision process to change master controller states. The grey box marks the rules based on the shape constrained splines method.

The master controller sets the pH setpoint to the high setpoint (6.8) when the nitrite concentration is such that the NOB are dominated by substrate limitation (i.e., open loop stable, Fig. 1 right, horizontally blue dashed area).

This is referred to as controller state 1. If nitrite is so high that the NOB are dominated by substrate inhibition (i.e., open loop unstable, Fig. 1 right, vertically orange dashed area) the controller sets the pH to the low setpoint (6.1). This is further referred to as controller state 0. The drift in the controller input signal forces to design the controller such that it relies on the information contained in the first and second derivative of the signal to distinguish between NOB inhibitory and NOB limiting nitrite concentration levels. The information that is actually used in the controller is the identified presence of the inflection point in the downward trend (i.e., negative first derivative, second derivative sign switches from negative to positive). It is assumed, that in the period during which the inflection point appears μAOB is constant: First, at this time, the pH has already reached its low setpoint value and the influent composition is assumed constant, thus there are no changes in the FA concentration. Second, the temperature is assumed constant. Furthermore, it is assumed that AOB activity is almost insensitive to changes in the nitrite concentration at the nitrite concentration level where the μNOB starts to be dominated by substrate limitation (Fig. 1, $\mathrm{TNN_{max}}$) (Wang et al., 2014). Consequently, when the inflection point appears, the nitrite dynamics are only driven by the NOB.

When NOB are dominated by substrate inhibition and a low pH results in low FA availability for AOB (Fig. 1, right, pink dotted line), the NOB activity increases as nitrite concentrations are decreasing (Fig. 1, moving from Point B to Point C). At the landmark value (Kuipers, 1986) $\mathrm{TNN_{max}}$, the

μNOB and in turn the net nitrite degradation rate reach their maxima and then start to decrease (Fig. 1, moving from Point C to Point A). Thus under normal circumstances, the appearance of the infection point in the decreasing signal is linked with the NOB achieving their maximum growth rate (point C) and the start of substrate limitation dominating the NOB. Note that the precise value of TNN_{max} is considered unknown.

Identifying an inflection point in the downward trend requires first and foremost that the nitrite concentration has been high enough to induce observable inhibition of the NOB. Thus, the controller has to be designed in such a way that NOB-inhibiting conditions are reached in a way that allows reducing the nitrite concentration as soon as inhibiting conditions are detected. Accordingly, the master controller increases the pH setpoint such that the increased FA concentration leads to an ammonia oxidation rate (i.e., nitrite production rate) higher than the maximal nitrite consumption rate (Fig. 1, right, purple dashed line). The nitrite increase is controlled by monitoring the absolute increase of the signal value. In our case, the last nitrite value prior to the pH increase is taken as a reference for a relative increase of 15 mg N/L. Once this threshold is reached the controller switches from state 1 to state 0.

In control state 0, the controller re-stabilises the process by decreasing the pH (Fig. 1, right, pink dotted line). As long as the nitrite concentration in the previous increase never exceeds point B (Fig. 1, right), the reduction in the FA concentration to the lower line puts the steady state concentration back to point A and a net nitrite reduction starts. The controller gets the confirmation of reaching a stable nitratation by identifying the inflection point in the downward trend. This ends one control cycle. Details concerning the practical implementation of this controller can be found in the Electronic Supplementary Material.

2.4. Identification of inflection point

To identify the inflection point in the downward nitrite signal, the signal is analyzed by means of a qualitative trend analysis (QTA) method. For this purpose, the shape-constrained spline function (SCS) method described in earlier works (Villez et al., 2013; Villez and Habermacher, 2016; Derlon et al., 2017; Mašić et al., 2017) is selected. The detailed modifications necessary for this work, particularly to enable online deployment, are described in the Electronic Supplementary Material. We illustrate the essence of this method next.

Fig. 3 illustrates two different time points in the analysis of the same event. The top panels show the data (black dotted) and the three shape-constrained spline models fitted to the data. These three models are increasingly flexible. One model (U) is constrained to be isotonic (monotonically increasing). The next model (UD) is constrained to exhibit a unimodal shape (single maximum, no minimum) with a concave profile after the identified maximum. The last model (UDA) has a unimodal shape also but is allowed to have a single inflection point after the identified maximum. The bottom panels show the corresponding root mean squared residual (RMSR) of the three models evaluated with all the data available until this time. In the left plot, the data already exhibited a maximum and the U model, constrained to be continuously increasing, starts to fit worse than the two other models. This can be seen in the almost flat shape the U model (red, wide-dashed) has from hour 6 on and thus results in an increasing RMSR of the U model ($\mathrm{RMSR_U}$). Both the UD and UDA models approximate the time series well as their shape constraints are flexible enough.

The right panel shows the time point at which the full data set of the event is available. Visual inspection reveals that the data exhibits a maximum and an inflection point in the downward trend - as expected. Shortly after hour 9 it becomes clear that a maximum is present in the time series given that $\mathrm{RMSR_U}$ increases dramatically. As desired, the $\mathrm{RMSR_{UD}}$ increases once the curve exhibits a convex form (hour 14), thus leading to the detection of the downward inflection point shortly after. A video illustrating the incremental data acquisition and concurrent data analysis can be found in the Electronic Supplementary Material.

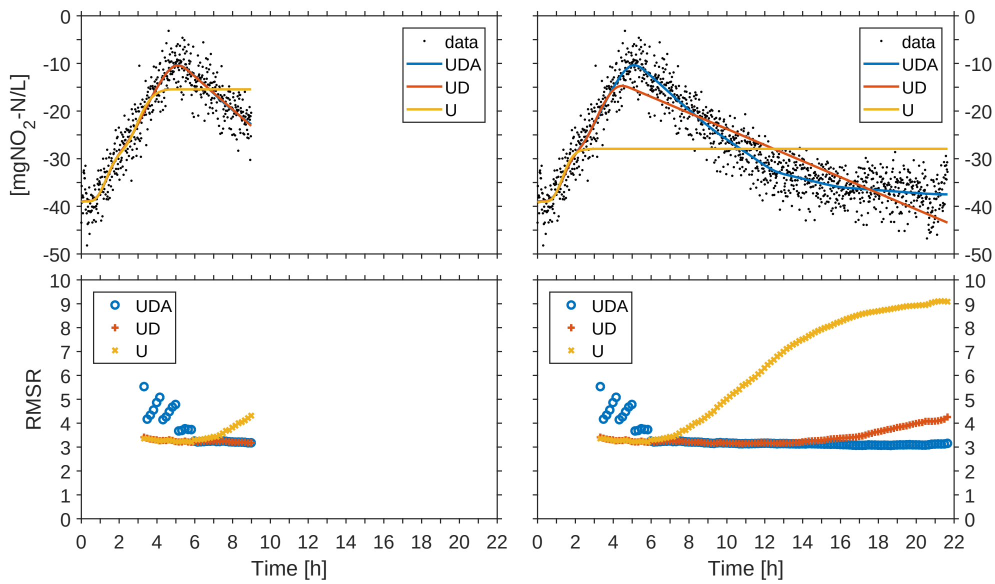

Figure 3: Shape constrained spline model fitting. Top panels: Raw data with three different qualitative sequence models fitted to the available data iduring an *event*. Bottom panels: Computed root mean squared residuals as a function of time. Left: Information available after 9h. Right: Information available at the end of the event.

2.5. Unmeasured process disturbances

Three unmeasured disturbances are tested or monitored to evaluate the robustness of the controller. First, the signal drift itself, which is expected to occur under any given practical operational condition. Thus, sensor drift is not actively induced but allowed to occur in a passive manner instead. Second, the robustness of the controller is tested against temperature dynamics and thirdly against influent composition dynamics.

2.5.1. Determination of drift rate

The nitrite reference measurements are compared with the estimation of the UV-Vis nitrite signal to monitor if the sensor signal actually drifts. The rate at which the difference of these two values change is the drift rate. Periods of drift are selected visually and then described by a piece-wise linear trend line. Drift is monitored in the whole experimental period (19.03.2018 - 30.05.2018, 72 days) including the periods in which the temperature and switch of influent source experiments (see below) take place.

2.5.2. Temperature experiments

In the ambient temperature range ($10 - 35$°C) the μAOB increases faster with temperature than the μNOB (Hellinga et al., 1998). To evaluate whether such disturbances pose a challenge to our control system the reactor is cooled or heated by means of the water based cooling and heating jacket. A *temperature low* experiment was executed twice. Each time the reactor was cooled down from 25°C to 22°C within 10-12 h and then heated back to 25°C within 10-12 h (16./17.04.2018 and 19./20.04.2018). A *temperature high* experiment was executed in two versions. In a long version (23.04.2018-25.04.2018), the temperature was increased within 8 h from 25 to 28°C, kept there for 36 h and then cooled down back to 25°C within 10 h. For the two short version experiments (26.04.2018 and 27.04.2018), the temperature was raised from 25 to 28°C within 10 h and then immediately cooled back to 25°C within 10 h. Note that these temperatures are typical for indoor applications and subtropical regions of the world.

2.5.3. Switch of influent source

Changes in the feed composition are another source of unmeasured process disturbances. To evaluate whether the controller is robust to this type of disturbances, we devised an experiment in the reactor feed compisition is changed deliberately. On April 30th, 2018 at 09:13, the influent was changed from source-separated urine collected from male toilets and urinals to source-separated urine collected from female toilets. Both female and male urine collection system are located in the Forum Chriesbach Building at Eawag Dübendorf in Switzerland. The urine from female toilets has a lower concentration of ammonia (-31%) and COD (-37%) due to dilution with flushing water in the NoMix toilets. A more comprehensive overview can be found in Fumasoli et al. (2016). More details can be found in the Electronic Supplementary Material (Table S2.1 and S2.2).

3. Results

3.1. Control behaviour

The following paragraph describes one control cycle during which the complete control system was in autonomous use (Fig. 4). At around 12:00, the controller state is 1 and the pH controller setpoint is 6.8 (*high pH setpoint*, 3$^{\text{rd}}$ panel). This induces an increase in nitrite, as expected (top panel). After reaching the threshold for a maximal difference to the previously defined baseline (i.e., *Rule 1*) the controller state is set to 0. The pH setpoint is reduced to 6.1 (*low pH setpoint*, 2$^{\text{nd}}$ panel). From this time on, the nitrite signal is recorded for analysis by the SCS models. After collecting the minimal number of nitrite measurements in this time series, the SCS models are fit for the first time. In the 4$^{\text{th}}$ panel one can see the incremental changes of the RMSR of the three different models U, UD, and UDA as new nitrite measurements are added to the analyzed data series. One can see that RMSR_{U} is always larger than RMSR_{UD} and RMSR_{UDA}. The interpretation is that the control algorithm recognises that the peak nitrite concentration has already occurred before this first time of comparative analysis. At 02:30 the RMSR_{UD} starts to deviate visually from the RMSR_{UDA}. The vertical line in the bottom panel indicates when *Rule 3* was evaluated as true shortly before 07:00, meaning that the controller now considers the presence of an inflection point in the nitrite signal as a sure thing. Shortly before 09:00 the 2 h timer *Rule 4* is also evaluated true and the controller switches back to state 1 (high pH setpoint). Consequently, the controller memorises the last nitrite value to reference the next nitrite increase and increases the pH setpoint to 6.8. This completes one autonomous cycle of the proposed controller.

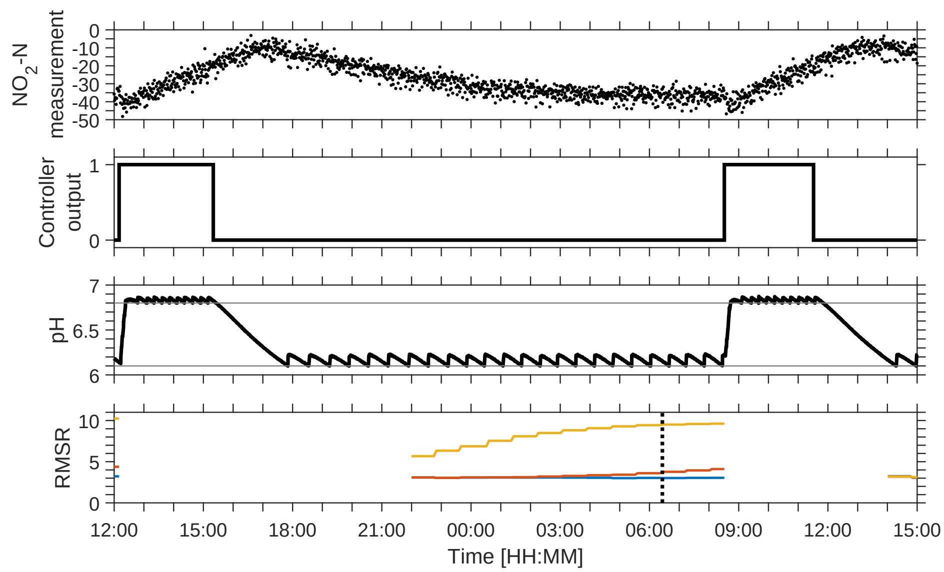

Figure 4: Operational data from one event as a function of time. 1st panel: Nitrite signal (controller input). 2nd panel: Controller state. 3rd panel: pH sensor signal with two setpoints. 4th panel: RMSR of the three fitted SCS models.

3.2. Controller performance

Fig. 5 illustrates nitrite end of cycle concentrations (ECC) measured after the detection of the inflection point but before the pH is increased again (T5, see Electronic Supplementary Material). The recorded ECC values represent substrate limiting conditions for the NOB during the complete experimental period. The ECC progressively decreased during the period of autonomous control. The solid retention time (i.e., equals the hydraulic retention time) never exceeds 13 days (Fig. 6 bottom panel) meaning that the experimental period covers more than 5.5 time the HRT (and SRT). Thus, the controller not only kept the nitrite concentration low in the short term, but also successfully prevented washout of the NOB population within a significant test period.

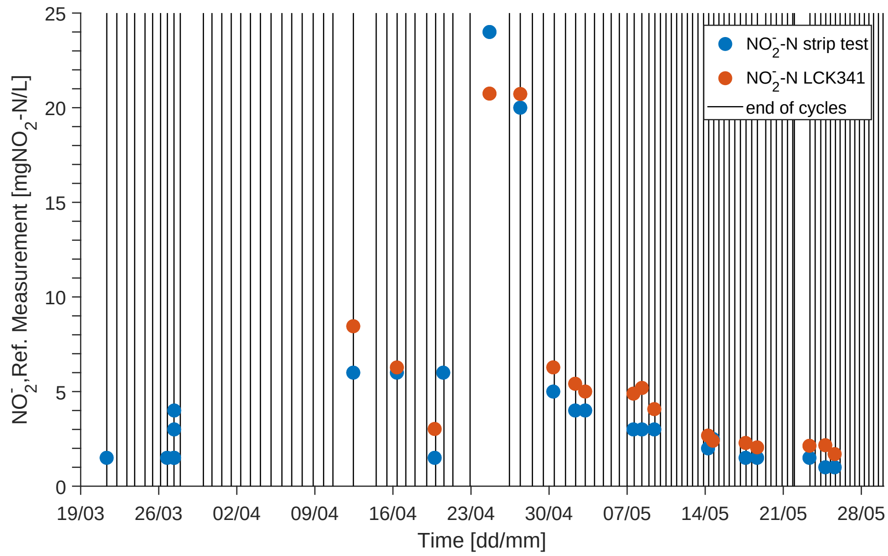

Figure 5: Nitrite end of cycle concentrations after identification of inflection point but before the start of next event (T5, see Electronic Supplementary Material). Vertical lines indicate the end of a cycle.

Despite the very noisy input signal, the visual inspection of the results reveals that the model selection by means of comparing the RMSRs of the three models has never resulted in a false negative or false positive identification of the maximum or the inflection point. It has to be noted that most likely there is a certain delay in the identification due to the chosen value for the knot distance. To quantify the delay, in every cycle the ground truth about TNN_{max} (Fig. 1) would need to be determined.

3.3. Unmeasured process disturbances

3.3.1. Drift

The controller input signal drift is illustrated in the top panel of Fig. 6. Drift occurred during the entire experimental period. The estimated drift rates, obtained with the fitted piece-wise linear trend line, range from - 0.8 to 1.1 mg NO_2^--N/L/d. Thus, one can conclude that the observed signal drift poses a meaningful challenge for process control, which has been mitigated successfully by the proposed control system. It is noted that the changes in the drift rates can only be explained partially. The vertical grey dashed lines indicate sensor cleaning. Sign changes of the drift rate are unexpected for this kind of intervention (i.e., a signal jump is expected when biofilm and solids are removed from the sensor.) Note that the initial difference between the UV-Vis based nitrite value and the nitrite reference measurements has been caused by drift in the 9 months in between the calibration period and the start of this study.

3.3.2. Switch of influent source

The change in influent composition (Fig. 6, 30.04.2018, yellow dashed line) induces a change in the sign of the drift rate from 1.1 to -0.4 mg N/L/d. In the first 15 days after the influent switch the ammonia and nitrate concentration in the reactor decrease from 2000 to 1300 mg N/L (Fig. 6, 2^{nd} panel). The controller reacted to the new lower concentrated influent and increased the hydraulic loading, which is indicated by the decreased hydraulic residence time (HRT) from around 13 to 7 days (Fig. 6, 3rd panel). Furthermore, also the control cycle length decreased from around 1 to 0.5 d (Fig. 5). Thus, the controller was able to reject this disturbance and keep nitrite levels low. At the same time, the slave controller was still acting as intended and compensated the decreased specific ammonia load with increased hydraulic loading.

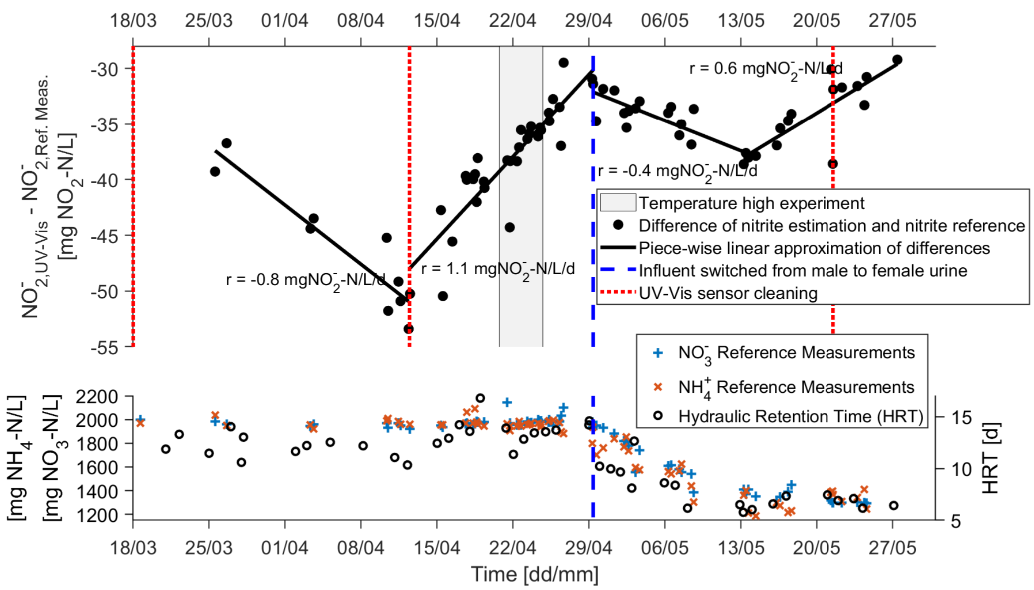

Figure 6: Drift rate, reactor nitrogen species concentrations, and hydraulic residence time. Top panel: deviations between the nitrite concentration signal and reference measurements as a function of time, piece-wise linear drift rate estimation, times of sensor cleaning, the time of influent source change from male to female urine, and the high temperature period. Bottom panel: Ammonia and nitrate concentrations in bulk and hydraulic retention time.

3.3.3. Temperature experiment

Fig. 7 shows the results of the temperature high experiment. The first complete cycle shown in this figure starts on April 21st and illustrates the operation before the temperature change. On April 22$^{\mathrm{nd}}$, the controller sets the pH setpoint to 6.8 (Fig. 7, 2$^{\mathrm{nd}}$ panel) before the temperature increase is visible (Fig. 7, 3$^{\mathrm{rd}}$ panel). The nitrite concentration rises for some time (Fig. 7, 1$^{\mathrm{st}}$ panel) while the temperature increases also. Shortly after, the controller decreases the pH setpoint while the temperature continues to increase. However, the nitrite signal remains at a high level (around -15 mg N/L) relative to the cycle before the temperature change (-30 mg N/L). Nitrite reference measurements confirm that elevated nitrite concentrations are the cause for this difference in the signal, which remain around 20 mg N/L instead of around 5 mg N/L as in the previous cycle. This very small drop in nitrite compared to the peak concentration, also leads to a delay in the identification of the inflection point (Fig. 7, 4$^{\mathrm{th}}$ panel) compared to the visual impression obtained by looking at the figure. The controller identified an inflection point only in the afternoon of April, 24$^{\mathrm{th}}$. An increase in pH at this time point would lead to an even higher accumulation of nitrite. To ensure successful testing of the controller against other disturbances, the controller is deactivated temporally (cf. grey area 2$^{\mathrm{nd}}$ panel) and the temperature setpoint is again decreased to 25°C. The cooling of the bulk media leads to a decrease in the nitrite starting at midnight on the 25$^{\mathrm{th}}$. At noon of the same day, the nitrite signal and reference measurements drop to the levels reached in the first cycle (Fig. 7, 22$^{\mathrm{nd}}$) and the controller is restarted shortly after. Thus, the temperature high experiment indicated that fast temperature increases pose a threat to the proposed control system. The temperature low experiment did not reveal any relevant finding with respect to the control performance. The only notable change compared to the 25°C operation is the reduction in the peak nitrite concentration by about 5 mg N/L.

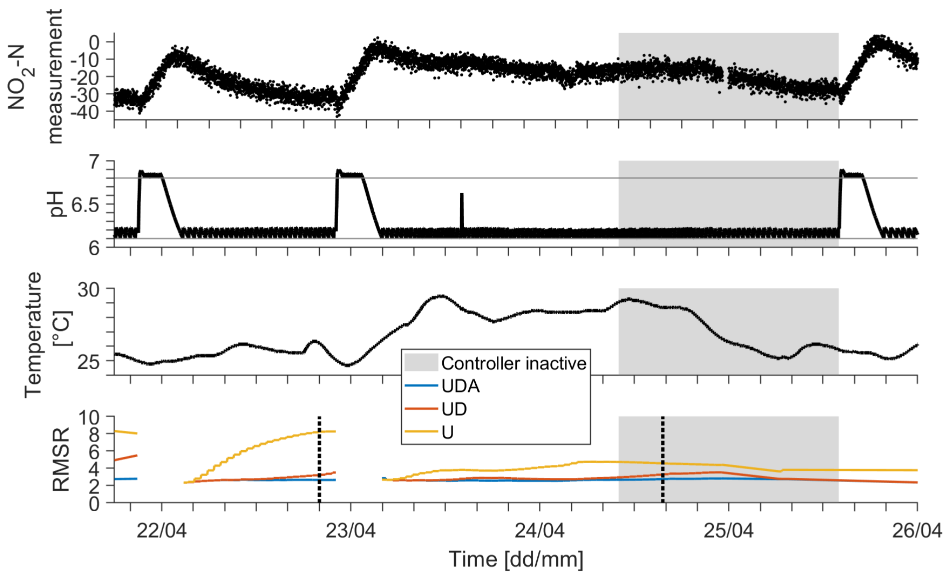

Figure 7: Temperature high experiment. 1st panel: Nitrite signal and nitrite reference measurements. 2nd panel: pH measurement. The grey area marks the period during which the controller was inactive. 3rd panel: Temperature measurement. 4th panel: RMSR of the three models U, UD, UDA including the time points at which the inflection point was identified.

4. Discussion

This study proposes a new concept for a stabilizing control in the presence of signal drift and demonstrates its utility by means of an intensive measurement campaign in a laboratory-scale reactor for urine nitrification.

The proposed control system avoids the effects of signal drift by using information in the first and second derivative to distinguish between stabilizing and destabilizing process conditions. The results reveal that the controller successfully stabilised the nitrification process despite using a sensor signal that is drifting permanently. Importantly, this could be achieved without redundant actuators or sensors and without a precise kinetic model of the process.

4.1. System performance

The end of cycle nitrite concentrations at the end of the control cycles were shown to decrease over time. This may indicate an adaption of the NOB to the elevated nitrite levels or could also be caused by the influent switch. Since steady state was not reached during the studied period, one cannot determine with absolute certainty whether the reported decrease is caused by a net decay of the AOB or a net growth of the NOB. Since the average pH in the reactor is higher than in the conventional operation with a constantly safe but low pH, this controller should theoretically also achieve higher nitrification rates (Udert and Wächter, 2012). However, pH is only one among many factors influencing the nitrification rates. Bürgmann et al. (2011) showed that long-term exposure to nitrite could jeopardise the process, while van Hulle et al. (2007) hypothesised that bacteria become more tolerant when exposed long enough to elevated nitrite concentrations. Consequently, future research should be aimed at understanding long-term reactor performance indicators in the presence of stabilizing control loops.

4.2. Unmeasured Disturbances

Our study shows that fast introduction of unmeasured disturbances can threaten the suitability of the proposed trend-based control concept. To understand why this is the case, one must note that the controller is based on the assumption that the appearance of an inflection point in the downward nitrite signal can only be explained by a change of from NOB-inhibiting to non-inhibiting nitrite concentration levels. To challenge this assumption as well as the control concept, two confounding factors were disturbed on purpose (temperature and influent composition).

The temperature increase experiment indicates that unmeasured disturbances can make the proposed control system fail. This is explained as an effect on the μAOB to μNOB ratio, which increases with temperature. Indeed, the fast temperature increase of the bulk media introduced the appearance of an inflection point. However, the assumption that the inflection point is solely caused by NOB dynamics does not hold any longer and explains the wrongful control action. While nitrite concentration does not yet reach the NOB-inhibiting region after one cycle, the early increase of the pH setpoint, induces an additional increase in the nitrite concentration. Such a higher concentration will likely inhibit the NOB and activate a positive feedback loop between the nitrite concentration, in turn inducing an increased risk of NOB wash-out in the long term. The temperature high experiment did reveal another important condition for correct functioning of the controller. The low amplitude of the signal (Fig. 7, 24^{th} afternoon) delays the identification of the inflection point. This shows the need for sufficient excitement of the process and the signal to reach a large enough signal-to-noise ratio. However, increased excitation also increases the risk of irreversible process failure (i.e., Fig. 1, exceed point B).

The influent switch experiment did not influence the observed signal profiles in a meaningful way. As a result, the controller was able to execute the right control actions in a timely manner throughout the course of this test. There are two explanations for this: First, the model to derive the nitrite concentrations from the UV-Vis absorbance measurement is apparently quite robust against changes in the reactor media composition, particularly large changes of the nitrate concentration (Fig. 6). Second, the dynamics caused by the influent switch are driven by the HRT and decreased from 13 to 7 d. Thus, this disturbance is much smoother than the temperature experiments with a time window of 0.5 d.

4.3. Extension of controller

The modifications applied to enable SCS analysis in an online environment worked without any complications. The main modification consisted of embedding the SCS as a model selection tool in a moving horizon estimation framework with a fixed start point. Despite concerns about the computational costs by Villez et al. (2013) the three SCS models could be fitted to the data within less than 3 seconds on an Intel® core i7 4970k 4 GHz processor. Thus, conventionally available computational resources are expected to be sufficient for most biochemical process monitoring applications. Faster computations, e.g. for fast processes or when dealing with high-frequency data collection systems, can be facilitated by increasing the knot distance of the spline functions. If computational cost is no concern at all, then the knot distance can be reduced to improve the fit of the applied SCS models.

So far, the controller makes the nitrite concentration oscillate around the optimal concentration for maximal μNOB. The upper setpoint has to ensure that nitrite is always accumulating to keep the signal informative. The lower setpoint has to ensure net nitrite degradation to stabilise the process. Choosing the setpoints can be challenging and some disturbances may influence the system such that the chosen pH setpoints cannot push the process into the intended operational region. Enabling the controller to decide how the two pH setpoints itself should be set would also facilitate process optimization.

One way to obtain a good ratio of the AOB activity to the NOB activity at both pH setpoints was revealed in the high temperature experiment. The increased temperature leads to a relatively high AOB rate at low pH. This in turn resulted in slow net nitrite degradation and thus a flat decreasing trend in the signal compared to the previous increase. Thus, the pH setpoints and in turn, the overall process performance, was rather high for the given NOB capacity. Potentially, computing the ratio of the increasing and the decreasing slope in one cycle allows optimizing the pH setpoints and in turn the process performance for the next cycle. Furthermore, using this kind of information would also help to reject additional disturbances without the need for additional instrumentation (cf. high temperature experiment).

4.4. Links to existing control theory

The proposed controller is based largely on a conceptual model of substrate affinity and inhibition in nitrifying bacteria. Assuming that the NOB activity, and thus also the nitrite conversion rate, has a unimodal shape with respect to the nitrite concentration, one can expect to observe an inflection point whenever the process shifts from conditions dominated by nitrite inhibition to conditions dominated by nitrite limitation. This information is key to avoid the need for any explicit correction of the signal drift since it is contained in the derivatives. Importantly, the actions taken by the controller can also be interpreted as the execution of an online experiment to determine the NOB kinetics. Microbial populations adapt over time and thus it is highly likely that the inhibition and affinity constants of these population change. Consequently, a sensor signal without relevant drift as input would allow tracking the optimal concentration of nitrite for a maximal μNOB.

This is also important with view on the many nitrification controllers equating nitrification with ammonia removal while nitrite oxidation is assumed to be completed simultaneously. Consequently, single indicators such as ammonia concentration, pH valley, or OUR drop have been assumed informative enough to control the process (Åmand et al., 2013; Jaramillo et al., 2018; Thürlimann et al., 2018). This is justifiable in some situations (e.g., municipal WWTP). However, in certain situations, analysis of both ammonia oxidation and nitrite oxidation is key for process stability and optimization. Partial nitritation/anammox (Lotti et al., 2012) or on-site WWTP, which can be limited by alkalinity are examples of this. We speculate that the proposed control concept can be used whenever derivatives are informative about the concentration trend of a relevant substance. The benefits of controllers executing online experiments to determine process states in continuously operated reactors are rarely studied in wastewater treatment. Steyer et al. (1999) also deliberately induced process disturbances to gain information about the performance of an anaerobic reactor. In contrast to the presented controller, they compared the information against a simple model to determine the performance.

The intentional excitement or perturbation of a system also has a theoretical basis in the form of extremum seeking control (ESC) (Liu and Krstic, 2012). Both ESC and the presented trend-based controller are model-free, feedback controllers that purposely excite the system to gain information. However, by default ESC requires an excitement frequency that is much lower than the dominant process frequency. This is not the case here as the biomass growth dynamics (HRT = 13 d) and the excitement frequency (1 d^{-1}) appear in the same time scale. Trollberg et al. (2014) found that the combination of a slow process and low excitement frequency as found in wastewater treatment make current forms of ESC impractical. They further stated that knowledge about the system behaviour close to the optimum is crucial to facilitate the use of ESC. Using ESC could however facilitate the inclusion of the ideas presented in 4.3. Thus, ESC may be helpful urine nitrification process optimization, in addition to ensuring long-term stability of the process.

5. Conclusion

In this study, a stabilizing controller for nitrification in high strength wastewater was developed and critically evaluated. The controller successfully prevents the occurrence of destabilizing nitrite accumulation events in an alkalinity limited urine nitrification reactor for the entire test period of 72 days. These are the main conclusions:

- Information contained in the derivatives of a drifting signal combined with qualitative knowledge about kinetics allowed for the control of an open-loop unstable system without the need for drift rate estimation or correction.

- Systems without any dynamics due to input or operation can be excited deliberately in such a way that the signal derivatives contain the information of interest about the process states. In this study, the controller was designed to destabilise the nitrification such that the signal derivatives contain the necessary information about the process state, in turn enabling stabilizing feedback control. Somewhat counter-intuitively, deliberate short-term destabilization facilitates the assurance of long-term process stability.

- The controller is based on a conceptual model of the process. This model currently excludes the effect of unmeasured disturbances other than the signal drift. This constitutes the most sensitive component of our proposed controller. Whereas slow unmeasured disturbances were successfully rejected, information in the controller input signal informing about fast, unmeasured disturbances were identified and considered for inclusion into the control logic.

Acknowledgement

The authors want to thank Benjamin Stucki and Kito Ohmura for their assistance with the experiments, Karin Rottermann and Sylvia Richter for their assistance with the laboratory analysis. Dominique Bonvin and Juan Pablo Carbajal for their inputs regarding the control theory. This research was made possible by the Swiss National Foundation (Project: 157097).

References

Åström, K.J., Murray, R.M., 2008. Feedback Systems: An Introduction for Scientists and Engineers. Princeton University Press, Princeton. OCLC: ocn183179623.

Al-Ghusain, I., Huang, J., Hao, O., Lim, B., 1995. Using pH as real-time control parameter for wastewater treatment and sludge digestion processes. Wat. Sci. Technol. 30(4), 159–168.

Åmand, L., Olsson, G., Carlsson, B., 2013. Aeration control Ű a review. Water Science and Technology 67, 2374–2398. doi:10.2166/wst.2013.139.

Baeza, J., Gabriel, D., Lafuente, J., 2002. In-line fast OUR oxygen uptake rate measurements for monitoring and control of WWTP. Water Science and Technology 45, 19–28.

Blanke, M., Kinnaert, M., Lunze, J., Staroswiecki, M., 2016. Diagnosis and Fault-Tolerant Control. 3rd ed. 2016 ed., Springer Berlin Heidelberg, Berlin Heidelberg.

Brito, R.S., Pinheiro, H.M., Ferreira, F., Matos, J.S., Lourenço, N.D., 2014. In situ UV-Vis spectroscopy to estimate COD and TSS in wastewater drainage systems. Urban Water Journal 11, 261–273.

Bürgmann, H., Jenni, S., Vazquez, F., Udert, K.M., 2011. Regime shift and microbial dynamics in a sequencing batch reactor for nitrification and anammox treatment of urine. Applied and Environmental Microbiology 77, 5897–5907. doi:10.1128/AEM.02986-10.

Derlon, N., Thürlimann, C.M., Dürrenmatt, D.J., Villez, K., 2017. Batch settling curve registration via image data modeling. Water Research 114, 327–337.

Etheridge, J.R., Birgand, F., Osborne, J.A., Osburn, C.L., Burchell, M.R., Irving, J., 2014. Using in situ ultraviolet-visual spectroscopy to measure nitrogen, carbon, phosphorus, and suspended solids concentrations at a high frequency in a brackish tidal marsh. Limnology and Oceanography: Methods 12, 10–22. doi:10.4319/lom.2014.12.10.

Fumasoli, A., Etter, B., Sterkele, B., Morgenroth, E., Udert, K.M., 2016. Operating a pilot-scale nitrification/distillation plant for complete nutrient recovery from urine. Water Science and Technology 73, 215–222.

Gruber, G., Bertrand-Krajewski, J.L., Beneditis, J.D., Hochedlinger, M., Lettl, W., 2006. Practical aspects, experiences and strategies by using UV/VIS sensors for long-term sewer monitoring. Water Practice and Technology 1.

Gujer, W., 2008. Systems Analysis for Water Technology. Springer-Verlag, Berlin Heidelberg.

Hellinga, C., Schellen, S.A.A.J.C., Mulder, J.W., van Loosdrecht, M.V., Heijnen, J.J., 1998. The SHARON process: an innovative method for nitrogen removal from ammonium-rich waste water. Water Science and Technology 37, 135–142.

Jaramillo, F., Orchard, M., Muñoz, C., Zamorano, M., Antileo, C., 2018. Advanced strategies to improve nitrification process in sequencing batch reactors - A review. Journal of Environmental Management 218, 154–164. doi:10.1016/j.jenvman.2018.04.019.

Kuipers, B., 1986. Qualitative simulation. Artif. Intell. 29, 289–338.

Liu, S.J., Krstic, M., 2012. Stochastic Averaging and Stochastic Extremum Seeking. Communications and Control Engineering, Springer-Verlag, London.

Lotti, T., van der Star, W.R.L., Kleerebezem, R., Lubello, C., van Loosdrecht, M.C.M., 2012. The effect of nitrite inhibition on the anammox process. Water Research 46, 2559–2569. doi:10.1016/j.watres.2012.02.011.

Mašić, A., Srinivasan, S., Billeter, J., Bonvin, D., Villez, K., 2017. Shape constrained splines as transparent black-box models for bioprocess modeling. Computers & Chemical Engineering 99, 96–105.

Ohmura, K., Thürlimann, C.M., Kipf, M., Carbajal, J.P., Villez, K., Submitted. Characterizing long-term wear of ion-selective ph sensors. DOI: 10.31224/osf.io/mv6tz [Preprint WWW Document].

Park, S., Bae, W., 2009. Modeling kinetics of ammonium oxidation and nitrite oxidation under simultaneous inhibition by free ammonia and free nitrous acid. Process Biochemistry 44, 631–640. doi:10.1016/j.procbio.2009.02.002.

Samuelsson, O., Björk, A., Zambrano, J., Carlsson, B., 2018. Fault signatures and bias progression in dissolved oxygen sensors. Water Science and Technology 78, 1034–1044. doi:10.2166/wst.2018.350.

Steyer, J.P., Buffière, P., Rolland, D., Moletta, R., 1999. Advanced control of anaerobic digestion processes through disturbances monitoring. Water Research 33, 2059–2068. doi:10.1016/S0043-1354(98)00430-8.

Sun, F.Y., Dong, W.Y., Shao, M.F., Li, J., Peng, L.Y., 2012. Stabilization of source-separated urine by biological nitrification process: Treatment performance and nitrite accumulation. Water Science and Technology: A Journal of the International Association on Water Pollution Research 66, 1491–1497. doi:10.2166/wst.2012.337.

Thürlimann, C.M., Dürrenmatt, D.J., Villez, K., 2018. Soft-sensing with qualitative trend analysis for wastewater treatment plant control. Control Engineering Practice 70, 121–133. doi:10.1016/j.conengprac.2017.09.015.

Thürlimann, C.M., Udert, K.M., Morgenroth, E., Villez, K., Submitted. Comparison of four methods to obtain calibration data for online nitrite estimation by means of in-line UV-Vis spectrophotometry. Water Research Submitted.

Trollberg, O., Carlsson, B., Jacobsen, E.W., 2014. Extremum seeking control of the CANON process – Existence of multiple stationary solutions. Journal of Process Control 24, 348–356. doi:10.1016/j.jprocont.2013.11.007.

Udert, K.M., Fux, C., Münster, M., Larsen, T.A., Siegrist, H., Gujer, W., 2003. Nitrification and autotrophic denitrification of source-separated urine. Water Science and Technology 48, 119–130.

Udert, K.M., Wächter, M., 2012. Complete nutrient recovery from source-separated urine by nitrification and distillation. Water Research 46, 453–464.

van Hulle, S.W.H., Volcke, E.I.P., Teruel, J.L., Donckels, B., van Loosdrecht, M.C.M., Vanrolleghem, P.A., 2007. Influence of temperature and pH on the kinetics of the Sharon nitritation process. Journal of Chemical Technology & Biotechnology 82, 471–480. doi:10.1002/jctb.1692.

Villez, K., Habermacher, J., 2016. Shape anomaly detection for process monitoring of a sequencing batch reactor. Computers & Chemical Engineering 91, 365–379.

Villez, K., Venkatasubramanian, V., Rengaswamy, R., 2013. Generalized shape constrained spline fitting for qualitative analysis of trends. Computers & Chemical Engineering 58, 116–134.

Wang, Q., Ye, L., Jiang, G., Hu, S., Yuan, Z., 2014. Side-stream sludge treatment using free nitrous acid selectively eliminates nitrite oxidizing bacteria and achieves the nitrite pathway. Water Research 55, 245–255. doi:10.1016/j.watres.2014.02.029.